

Lawrence Berkeley National Laboratory

Recent Work

Title

BASIC THEORY AND APPLICATION OF REGGE POLES

Permalink

<https://escholarship.org/uc/item/3f17b2hq>

Authors

Jones, C. Edward
Poirer, John A.

Publication Date

1963-02-08

UCRL-10677
C.2

University of California
Ernest O. Lawrence
Radiation Laboratory

TWO-WEEK LOAN COPY

*This is a Library Circulating Copy
which may be borrowed for two weeks.
For a personal retention copy, call
Tech. Info. División, Ext. 5545*

BASIC THEORY AND APPLICATION
OF REGGE POLES

Berkeley, California

10677
C.2.

DISCLAIMER

This document was prepared as an account of work sponsored by the United States Government. While this document is believed to contain correct information, neither the United States Government nor any agency thereof, nor the Regents of the University of California, nor any of their employees, makes any warranty, express or implied, or assumes any legal responsibility for the accuracy, completeness, or usefulness of any information, apparatus, product, or process disclosed, or represents that its use would not infringe privately owned rights. Reference herein to any specific commercial product, process, or service by its trade name, trademark, manufacturer, or otherwise, does not necessarily constitute or imply its endorsement, recommendation, or favoring by the United States Government or any agency thereof, or the Regents of the University of California. The views and opinions of authors expressed herein do not necessarily state or reflect those of the United States Government or any agency thereof or the Regents of the University of California.

UCRL-10677
UC-34 Physics
TID-4500 (19th Ed.)

UNIVERSITY OF CALIFORNIA
Lawrence Radiation Laboratory
Berkeley, California

Contract No. W-7405-eng-48

BASIC THEORY AND APPLICATION OF REGGE POLES

C. Edward Jones and John A. Poirer

February 8, 1963

Printed in USA. Price \$1.00. Available from the
Office of Technical Services
U. S. Department of Commerce
Washington 25, D.C.

BASIC THEORY AND APPLICATION OF REGGE POLES

Contents

Abstract	v
I. Introduction	1
II. Background	2
III. Analytic Continuation in Angular Momentum	4
IV. Elementary Particles and Resonances	6
V. Sommerfeld-Watson Transformation	8
VI. High-Energy Scattering	10
VII. Signature of Regge Trajectories	11
VIII. Pomeranchon	12
IX. Relations Between Total Cross Sections	15
X. Angular Distributions	16
XI. Total Elastic Cross Sections	18
XII. Isolating Regge Trajectories	19
XIII. Backward and Charge-Exchange Scattering	26
Appendices	
A. Exchange Scattering	29
B. Ordinary Diffraction Scattering	30
References	31

BASIC THEORY AND APPLICATION OF REGGE POLES

C. Edward Jones and John A. Poirier

Lawrence Radiation Laboratory
University of California
Berkeley, California

February 8, 1963

ABSTRACT

This paper gives a development of the basic theory of Regge poles. The goal has been to give a self-contained discussion which can be easily read without prior background knowledge of the subject. Emphasis is on physical ideas and experimental consequences rather than on rigor. The attempt has been made to state explicitly the underlying assumptions behind the Regge pole hypothesis.

BASIC THEORY AND APPLICATION OF REGGE POLES*†

C. Edward Jones and John A. Poirier

Lawrence Radiation Laboratory
University of California
Berkeley, California

February 8, 1963

I. INTRODUCTION

In recent months, a new insight has been gained into elementary-particle-scattering problems, as a result of the work of Regge.^{1,2} Regge studied the scattering of particles in ordinary quantum mechanics with a potential and found (a) that the partial-wave amplitudes which express the scattering in states of well-defined angular momentum could be defined for all values of the angular-momentum variable l in the complex plane, instead of just for positive integers; and (b) that, considered as analytic functions of the variable l , these same amplitudes have simple poles located in the complex l plane. Attempts have since been made to generalize the results of Regge and to assume that such angular-momentum poles also exist in relativistic scattering.^{3,4} The purpose of this paper is to describe in a simple way the essential features of these latter attempts, developing the subject from the beginning.

The point of view that we shall take in what follows is to assume the existence of Regge poles in relativistic scattering and then to explore the physical consequences of this assumption. We shall emphasize how the Regge pole hypothesis leads to observable predictions. The reader is referred to the work of Regge,^{1,2} for rigorous proofs of the existence of Regge poles in potential scattering. In the relativistic case, the rigorous analyticity properties of the scattering amplitudes in the variable l are still under investigation.

According to recent studies, there may be branch cuts in the angular-momentum plane; that is, branch points in the variable l .⁵ We have ignored this possibility here and have considered only simple poles in l . It should be borne in mind that the existence of such cuts could, depending upon their locations and movements, complicate considerably the picture given here.

It is hoped that the discussion of Regge poles presented herein will provide the background for easy access to the current literature on this subject.

* Work done under the auspices of the U. S. Atomic Energy Commission.

† This paper is an outgrowth of a series of informal talks given by one of us (C. E. J.) to the Moyer Group at the Lawrence Radiation Laboratory, Berkeley.

II. BACKGROUND

Let us first write down the differential cross section in the center-of-mass (c. m.) system for the elastic scattering of two particles:

$$\frac{d\sigma}{d\Omega} = |f(E, \cos \theta)|^2, \quad (1)$$

where E is the total energy in the c. m. and θ is the c. m. scattering angle.

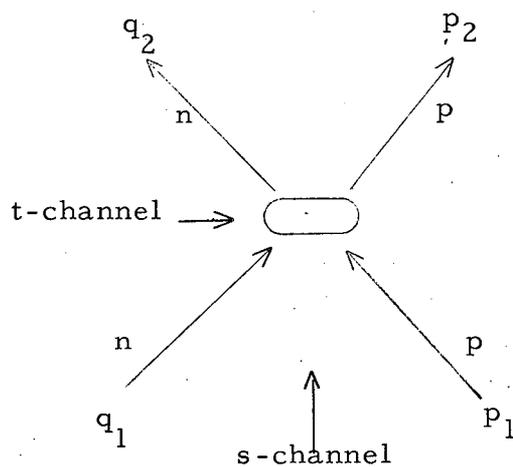


Fig. 1. Scattering of $n+p \rightarrow n+p$.

Let us take as a concrete example np (neutron-proton) scattering (Fig. 1), where q_1, q_2 are the initial and final four-momenta for the neutron and p_1, p_2 are the corresponding quantities for the proton. We define two new variables s and t :

$$s = (q_1 + p_1)^2, \quad (2)$$

$$t = (q_1 - q_2)^2. \quad (3)$$

Since these variables are squares of four-vector quantities, they are Lorentz-invariant.

We now evaluate the variables s and t in terms of E and θ . In the c. m. frame for neutron-proton scattering $q_1 = -\vec{p}_1$, where $\vec{}$ denotes the ordinary three-momentum vector. For the case of equal masses, $q_1^2 = q_2^2 = p_1^2 = p_2^2$, which we denote simply by \vec{q}^2 . Therefore we can write

$$s = (q_1 + p_1)^2 = (q_2 + p_2)^2 = q_1^2 + p_1^2 + 2q_1 \cdot p_1 = 4(\vec{q}^2 + M^2) = E^2,$$

$$t = (q_1 - q_2)^2 = (p_2 - p_1)^2 = q_1^2 + q_2^2 - 2q_1 \cdot q_2 = -2\vec{q}^2(1 - \cos \theta). \quad (4)$$

The range of physical values for the variables s and t is

$$\left. \begin{array}{l} -4\vec{q}^2 < t \leq 0 \\ 4M^2 < s \end{array} \right\} \text{Region I.} \quad (5)$$

where $\vec{q}^2 = \frac{s}{4} - M^2$

When the variables s and t are in this range, we shall say that we are in Region I, or the physical region for the np channel. The process $n+p \rightarrow n+p$ is called the "s-channel" of the diagram in Fig. 1, s being the square of the total c.m. energy for this process. It is customary to define a Lorentz-invariant function $A(s, t)$, which is called the invariant scattering amplitude and is defined by⁶

$$A(s, t) = \frac{\sqrt{s}}{2} f(E, \theta) . \quad (6)$$

Here $A(s, t)$ is assumed to be an analytic function of the variables s and t except for specified poles and branch point singularities. Being an analytic function, $A(s, t)$ is well-defined by analytic continuation outside of Region I.

For instance, we can consider Region II defined by

$$\left. \begin{array}{l} 4M^2 < t \\ -4\vec{q}_t^2 < s < 0 \end{array} \right\} \text{Region II.} \quad (7)$$

where $\vec{q}_t^2 = \frac{t}{4} - M^2$

The principle of crossing symmetry⁶ tells us that $A(s, t)$ with the variables in the range defined by Region II represents the invariant scattering amplitude in the c.m. frame for the process $n + n \rightarrow p + \bar{p}$. This is the "t-channel" for the diagram in Fig. 1, and \vec{q}_t is the c.m. three-momentum. It can be noted that we have simply viewed the diagram in Fig. 1 from the side and changed particle to antiparticle whenever we have gone against an arrow. Further, t is now the total c.m. energy squared for the $\bar{n}n$ system and s is related to the angle, θ_t , between incident n and final \bar{p} by

$$s = -2\vec{q}_t^2 (1 - \cos \theta_t) . \quad (8)$$

The four-momentum of the incident \bar{n} is $-q_2$, and for the final state \bar{p} is $-p_1$ (see Fig. 2).

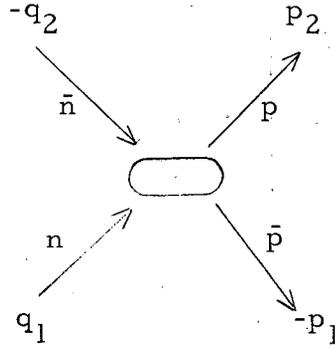


Fig. 2. Crossed channel for $n + p \rightarrow n + p$.

Also one usually defines the u-channel process, which for this case is $n + \bar{p} \rightarrow n + \bar{p}$; the u-channel will not be used explicitly in this paper.

We record here for future use the Cauchy Residue Theorem for an analytic function $f(z)$ with poles located at points $z = z_i$,

$$\oint_C f(z) dz = 2\pi i \sum_i \text{residue} [f(z_i)] , \quad (9)$$

where the counterclockwise contour of integration, C , encloses poles of f .

III. ANALYTIC CONTINUATION IN ANGULAR MOMENTUM

We now perform a standard partial-wave decomposition in Region I:

$$A(s, t) = \sum_{\ell=0}^{\infty} (2\ell + 1) A_{\ell}^s(s) P_{\ell}(\cos \theta), \quad (10)$$

and in Region II

$$A(s, t) = \sum_{\ell=0}^{\infty} (2\ell + 1) A_{\ell}^t(t) P_{\ell}(\cos \theta_t), \quad (11)$$

where in Region II the roles of s and t are interchanged. In terms of phase-shift notation $A_{\ell}^t(t)$ is (for the case of equal masses)

$$A_{\ell}^t(t) = \sqrt{\frac{\vec{q}_t^2 + M^2}{\vec{q}_t^2}} \exp i\delta_{\ell}(t) \sin \delta_{\ell}(t). \quad (12)$$

Of course, $A_{\ell}^t(t)$ is defined only for positive integer values of ℓ . Let us suppose a function $A(\ell, t)$ exists with the following properties: (a) it is an analytic function of ℓ defined for all complex values of ℓ , and (b) $A(\ell, t) = A_{\ell}^t(t)$ whenever ℓ is a positive integer. Thus $A(\ell, t)$ coincides with the usual partial-wave amplitude when ℓ is a positive integer but is now also defined for all values of ℓ in the complex plane. (See reference 7.)

Regge showed that in potential scattering (nonrelativistic Schrödinger equation)^{1, 2} that it is possible to so define an $A(\ell, t)$ for complex ℓ . In the Schrödinger equation, the fact that ℓ is an integer results from boundary conditions that are placed on the wave function to obtain physical solutions. If these conditions are relinquished, solutions are known to exist for all ℓ .^{1, 2} (It was known previously that $P_{\ell}(\cos \theta)$ could be defined for noninteger values of ℓ and non-real values of $\cos \theta$). Regge further showed that in potential theory $A(\ell, t)$ can be written

$$A(\ell, t) = \frac{N(\ell, t)}{D(\ell, t)}, \quad (13)$$

where N and D are analytic functions of ℓ and t for $\text{Re } \ell > -1/2$, and N has no poles. Therefore the conditions

$$D(\ell, t) = 0 \quad (14)$$

gives the location of the poles in $A(\ell, t)$. Solving Eq. (14) for ℓ we obtain

$$\ell = \alpha(t). \quad (15)$$

Thus $A(\ell, t)$ has a pole in the ℓ plane at $\ell = \alpha(t)$. The following important points should be noted: (a) The pole in the ℓ plane specified by Eq. (15) moves as t changes. (b) If Eq. (15) is inverted we can also view the pole as occurring in the variable t but moving with ℓ . (c) The poles given by Eq. (15) are the only singularities in ℓ . Poles in angular momentum which move with energy are called Regge poles.

Now we make a leap from potential theory to relativistic amplitudes and assume that they too have these same properties. Much of this leap has not been proved but, to the extent that we think of nonrelativistic theory as being a limit of the relativistic theory, one might expect that the leap is a reasonable thing to try.

IV. ELEMENTARY PARTICLES AND RESONANCES

The Regge poles in $A(\ell, t)$ have a simple physical meaning. Let us expand $A(\ell, t)$ in a series where the first term gives the pole behavior

$$A(\ell, t) = \frac{\beta_i(t)}{\ell - a_i(t)} + \dots \quad (16)$$

Next we expand the real part of a_i about a point t_r ,

$$a(t) = \text{Re } a(t_r) + \text{Re } a'(t_r)(t - t_r) + i \text{Im } a(t_r). \quad (17)$$

Then Eq. (16) becomes

$$A(\ell, t) = \frac{\beta(t)}{\ell - \text{Re } a(t_r) - \text{Re } a'(t_r)(t - t_r) - i \text{Im } a(t_r)}, \quad (18)$$

where we have suppressed the subscript i . Suppose that $\text{Re } a(t_r)$ is equal to a positive integer as shown in Fig. 3. Now look at the partial wave $\ell = \text{Re } a(t_r) = \text{integer}$.

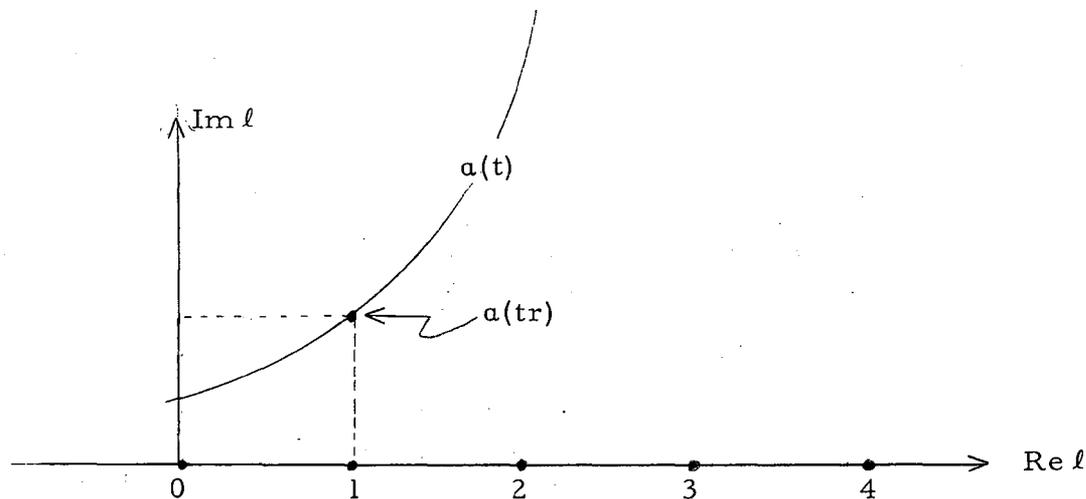


Fig. 3. Location of the pole in ℓ as t varies.

For this case

$$A(\ell, t) = \frac{\beta(t) / -\operatorname{Re} a' (t_r)}{(t-t_r) + i \frac{\operatorname{Im} a(t_r)}{\operatorname{Re} a' (t_r)}}, \quad (19)$$

where we have divided the numerator and denominator of Eq. (18) by $-\operatorname{Re} a' (t_r)$. We recognize Eq. (19) as a Breit-Wigner resonance formula with a resonance at $t=t_r$ (phase shift going through 90 deg), with a width Γ , given by

$$\Gamma = \frac{+\operatorname{Im} a(t_r)}{\operatorname{Re} a' (t_r)}. \quad (20)$$

Therefore we see a resonance in the wave when $t=t_r$, or alternatively when $\operatorname{Re} a =$ positive integer. In the example pictured, we have a p-wave resonance. If we assume that a' is not a strong function of t , then the width of the resonance is proportional to $\operatorname{Im} a(t_r)$. If $\operatorname{Im} a(t_r) = 0$ at an integer ℓ , then $\Gamma=0$ (or $\tau=\infty$) and we would interpret this as a stable elementary particle or bound state.

The Regge pole hypothesis for systems of strongly interacting particles can now be simply stated: All particles and resonances, stable or unstable, lie on Regge trajectories. In some cases more than one observed particle and/or resonance may lie on the same trajectory. The trajectories are characterized by a complete set of quantum numbers excluding, of course, mass and spin, which change along the trajectory. This concept of particles and resonances leads one to say that there are no elementary particles, since after all they are merely points on a trajectory with no part of the trajectory being any more fundamental or elementary than any other.^{3, 4}

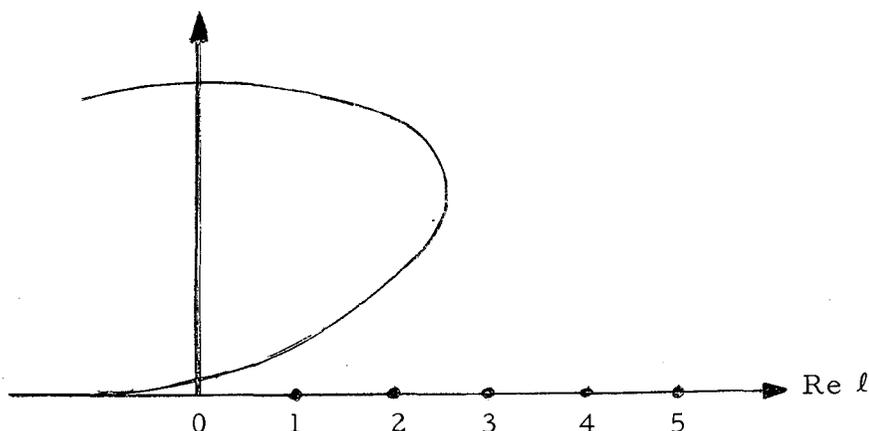


Fig. 4. Behavior of the pole in ℓ in potential theory.

Figure 4 is a sketch of the probable behavior of $a(t)$. This shape can be derived for the Yukawa potential.⁸ The upper part of the curve, which swings back, does not produce an observable resonance because the width is too broad.

V. SOMMERFELD-WATSON TRANSFORMATION

The next step is to express $A(s, t)$ as a contour integral:

$$A(s, t) = - \frac{1}{2i} \int_C \frac{d\ell (2\ell+1) A(\ell, t) P_\ell[-\cos \theta_t]}{\sin \pi \ell} \quad (21)$$

where the path of the line integral, C , is defined in Fig. 5 below. This will be seen to reduce to Eq. (11). The contour is drawn so as to exclude all singularities in $A(\ell, t)$ even if they should occur near the horizontal axis.

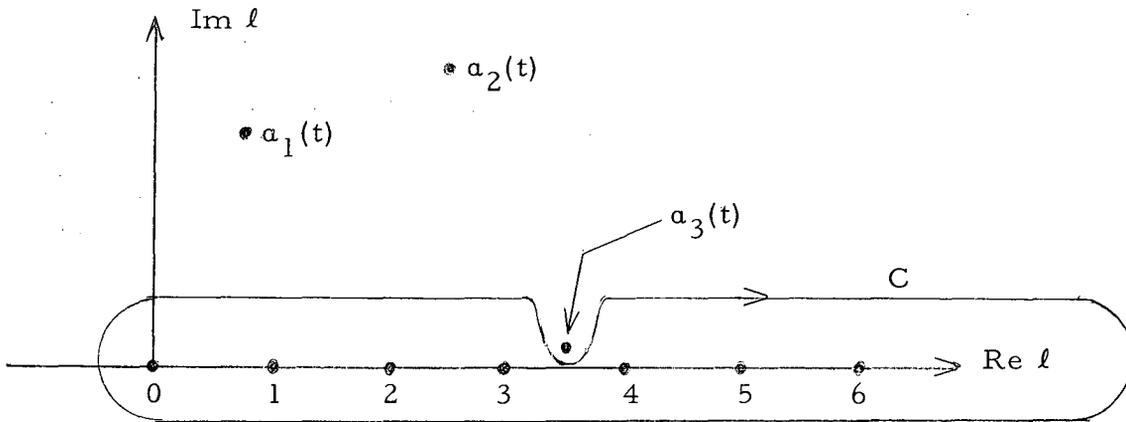


Fig. 5. Contour in the complex ℓ -plane.

This particular transformation is known as the Sommerfeld-Watson transform.⁹ One can see that Eq. (21) yields the same result as Eq. (11) by noting that (a) all singularities except those in $1/\sin \pi \ell$ are excluded by the contour; (b) the singularities of $1/\sin \pi \ell$ have a residue of $(-1)^\ell / \pi$ at each integer value of ℓ ; (c) $P_\ell(-\cos \theta) = (-1)^\ell P_\ell(\cos \theta)$ for positive integer ℓ ; and (d) the path of integration in Fig. 5 is clockwise whereas the Cauchy theorem [Eq. (9)] is counterclockwise, which introduces an extra minus sign.

VI. HIGH-ENERGY SCATTERING

We shall now use the Regge pole hypothesis to study high-energy scattering. We recall that Eq. (22) was derived from Eq. (11), which is an expansion in Region II, or the t-channel (see Fig. 1). We would like now to go to the s-channel in Region I [Eqs.(5)]. Using Eq. (22), let us investigate the asymptotic behavior of A , σ^{tot} , and $d\sigma/d\Omega$, as s approaches infinity.

The first term is a contour integral over the vertical line in the complex ℓ plane $\text{Re } \ell = -1/2$. The behavior of the integral as a function of s is determined by the asymptotic behavior of the Legendre polynomial¹⁰

$$P_a(z) \rightarrow z^a \text{ as } z \rightarrow \infty \text{ for } \text{Re } a \geq -\frac{1}{2}, \quad (23)$$

so that

$$P_\ell(-1 - s/2q_t^2) \rightarrow (-s/2q_t^2)^\ell \text{ for } s \rightarrow \infty. \quad (24)$$

The asymptotic behavior in s of the integral $\int d\ell (2\ell+1)A(\ell, t)P_\ell(-1 - s/2q_t^2)$ taken along the line $\text{Re } \ell = -1/2$ is seen to be $\lesssim (-s/2q_t^2)^{-1/2}$, which goes to zero as $s \rightarrow \infty$. Therefore only the sum term in Eq. (22) contributes to the asymptotic behavior of $A(s, t)$ as $s \rightarrow \infty$. Recall that the i th Regge pole occurs at $\ell = \alpha_i(t)$ and has a residue of $\beta_i(t)$. The Regge poles in Eq. (22) correspond to resonances in the t-channel. Thus these poles or resonances in the t-channel control the high-energy behavior of the scattering amplitude in the s-channel. We are discussing Region I where $t < 0$ so that we are below the physical threshold for the t-channel. When t is less than threshold it is generally believed that $\text{Im } \alpha(t) = 0$. It is clear that if $\alpha(t)$ passes through a positive integer for t less than threshold, $\text{Im } \alpha(t)$ is zero, for this pole must correspond to a bound particle (infinite lifetime). That $\text{Im } \alpha(t) = 0$ for all values of $\alpha(t)$ when t is less than threshold can be proved in potential scattering¹¹ (except for unusual cases) and we shall assume this property here. With these comments we now write the asymptotic behavior of Eq. (22):

$$A(s, t) \rightarrow - \sum_i (-s/2q_t^2)^{\alpha_i} \beta_i(t) \pi(2\alpha_i + 1) / \sin \pi \alpha_i \text{ for } s \rightarrow \infty. \quad (25)$$

Let us plot the $\text{Re } \alpha$ as a function of t (see Fig. 7).

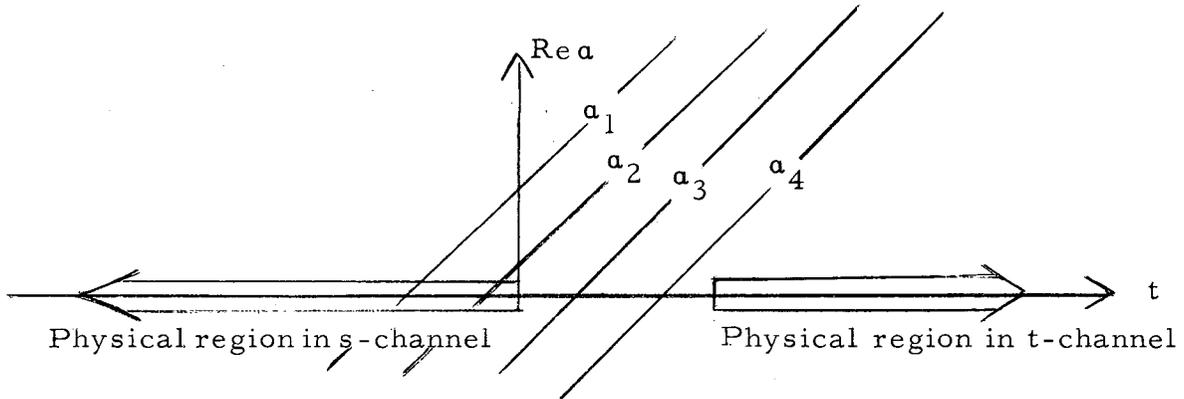


Fig. 7. t-channel poles, which contribute to high s-behavior.

In this sum over i terms, the whole sum will be dominated at large s by the term having the largest value of a_i .

VII. SIGNATURE OF REGGE TRAJECTORIES

In potential theory when there is an exchange potential there are, in effect, two different potentials acting: one for the even partial waves, and one for the odd. (See Appendix A.)

Thus a Regge pole term $R(s, t)$ enters the amplitude in one of two forms

$$R(s, t) = -\pi [2\alpha(t) + 1] \beta(t) \frac{P_\alpha(\xi) \pm P_\alpha(-\xi)}{2 \sin \pi\alpha} \quad , \quad (26)$$

where

$$\xi = -1 - s/2q_t^2 \quad .$$

The plus sign in Eq. (26) corresponds to a Regge trajectory with an even signature, the minus sign corresponds to odd signature. Thus depending on the signature, a Regge pole term contributes either to odd or even waves, not both. It is important to note that if α approaches an odd integer for an even-signature Regge pole (that is, one carrying plus sign above), $R(s, t)$ does not approach zero since the denominator also vanishes. If α approaches an even integer for an even-signature Regge pole then $R(s, t)$ behaves in this vicinity as

$$R(s, t) \approx \frac{\pi [2\alpha(t) + 1] \beta(t) P_\alpha(\xi)}{\sin \pi\alpha(t)} \quad , \quad (27)$$

and $A(s, t)$ has a pole. Regge poles in relativistic scattering are also assumed to have well-defined signatures,¹² and thus the trajectories can define a particle or resonance state only at every other integer value of $\text{Re } \ell$.¹³

VIII. POMERANCHON

Now we want to see what would happen if the highest trajectory [and hence the one that will dominate the sum in Eq. (27) for large s] has even signature. We must then take the symmetric combination of Legendre polynomials from Eq. (26):

$$A(s, t) \rightarrow \frac{-\pi(2\alpha+1)\beta(t)}{2 \sin \pi\alpha} (P_\alpha(-z) + P_\alpha(+z)), \quad (28)$$

where we have picked the α_i that dominates the sum.

From Eq. (23) the asymptotic behavior of the last term in Eq. (28) is

$$P_\alpha(-z) + P_\alpha(z) \rightarrow (-z)^\alpha + z^\alpha \text{ as } z \rightarrow \infty, \quad (29)$$

which can be rewritten

$$(s/2\vec{q}_t^2)^\alpha (1 + e^{-i\pi\alpha}) = (s/2\vec{q}_t^2)^\alpha (1 + \cos \pi\alpha - i \sin \pi\alpha). \quad (30)$$

Putting this symmetrized version of P_α into Eq. (25) we get

$$A(s, t) \xrightarrow{s \rightarrow \infty} -(1/2) \frac{(s/2\vec{q}_t^2)^\alpha (1 + \cos \pi\alpha - i \sin \pi\alpha) \beta(t) \pi(2\alpha+1)}{\sin \pi\alpha}. \quad (31)$$

From the optical theorem we relate $\text{Im } A(s, 0)$ to the total cross section,

$$\text{Im } A(s, 0) = |\vec{q}| \sqrt{s} \sigma^{\text{tot}}/8\pi. \quad (32)$$

From Eq. (31),

$$\text{Im } A(s, t) \xrightarrow{s \rightarrow \infty} \left(\frac{1}{2}\right) (s/2\vec{q}_t^2)^\alpha \beta(t) \pi(2\alpha+1), \quad (33)$$

which we will write as

$$\text{Im } A(s, t) \xrightarrow{s \rightarrow \infty} b(t) s^\alpha, \quad (34)$$

where $b(t)$ incorporates the t dependence of Eq. (33) and is independent of s . Noting that $|\vec{q}|^2 \rightarrow s/4$ as $s \rightarrow \infty$ and setting $t = 0$, we obtain

$$\sigma^{\text{tot}} = 16 \pi b(0) s^{a(0)-1}, \text{ as } s \rightarrow \infty. \quad (35)$$

Experimentally it appears that all cross sections involving strong interactions approach constants at high energies. For σ^{tot} in Eq. (35) to be a constant at $s = \infty$, $a(0)$ must equal 1, with $a_i(0) \leq 1$ for all other trajectories. This Regge pole trajectory which passes through $\text{Re } \alpha = 1$ at $t = 0$ is called the Pomernanchuk trajectory or the Pomernanchon.^{3, 4} It is assumed to have the

quantum numbers of the vacuum. This is reasonable because this trajectory would then control the high-energy limit of all total cross sections and make them all tend to constants. It is interesting to note that the strongest forces (forces that lead to the most scattering) thus arise from the exchange of system(s) which have the quantum numbers of the vacuum. This general notion that "the simpler the quantum numbers the stronger the force" seems to hold qualitatively throughout all the Regge trajectories. For example the ρ -Regge trajectory appears to contribute the next highest power of the scattering under the Pomeron, and its quantum numbers differ from the vacuum only in isotopic spin and spatial parity, (see Fig. 8).

Let us see what would happen if the signature of this highest Regge trajectory were odd. Going back to Eq. (28) and rederiving its asymptotic behavior we must take the combination $[P_\alpha(-z) - P_\alpha(+z)]$. Equation (31) now becomes, for odd signature,

$$A(s, t) \xrightarrow{s \rightarrow \infty} \frac{\left(\frac{1}{2}\right) (s/2q_t^2)^\alpha (1 - \cos \pi\alpha + i \sin \pi\alpha) \beta(t) \pi (2\alpha + 1)}{\sin \pi\alpha} \quad (36)$$

When $\alpha \rightarrow 1$, $\text{Re } A \rightarrow \infty$. This would mean that the elastic cross section would become infinite. Since this cannot happen, we conclude that the highest Regge trajectory must have even signature.

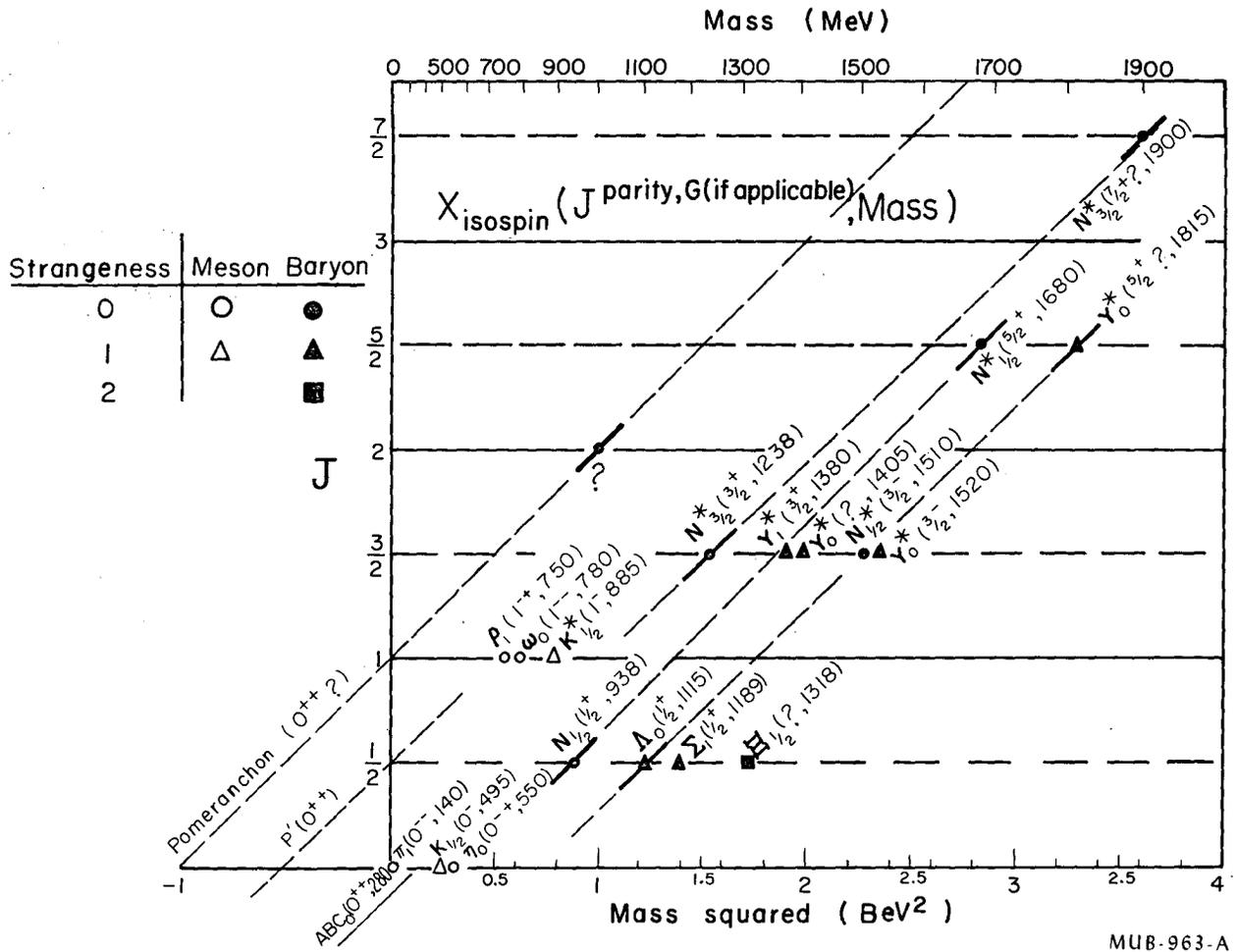
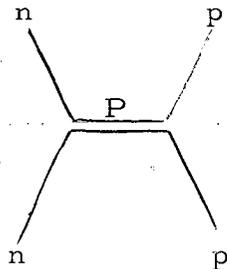


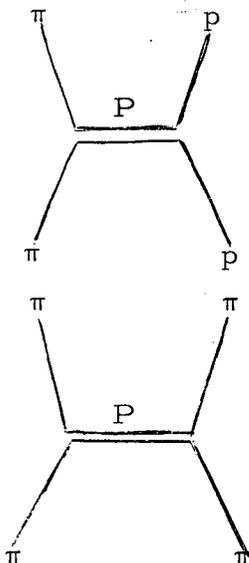
Fig. 8. Regge trajectories on a Chew-Frautschi plot.
 (We are indebted to A. H. Rosenfeld for this graph.)

IX. RELATIONS BETWEEN TOTAL CROSS SECTIONS

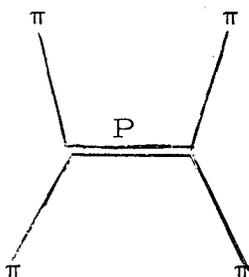
A prediction of the total cross section for $\pi\pi$ scattering at high energies is an example of some further results that can be obtained from the theory. Since b is essentially the residue of a pole in the scattering amplitude, we write the following:



$b_1(0) \propto (\gamma_{PN\bar{N}})^2$ where γ denotes the coupling between the Pomeranchon and a nucleon-antinucleon pair (N denotes a nucleon, P denotes Pomeranchon),



$b_2(0) \propto \gamma_{P\pi\pi} \gamma_{PN\bar{N}}$,



$b_3(0) \propto (\gamma_{P\pi\pi})^2$,

where we realize that $\sigma^{\text{tot}} \propto b(0)$. From these relationships we obtain that

$$\sigma^{\text{tot}}(\pi\pi) = [\sigma^{\text{tot}}(\pi p)]^2 / \sigma^{\text{tot}}(pp) \tag{37}$$

in the limit of high energies. It might be interesting to put in some experimental numbers at this point.

$$\sigma^{\text{tot}}(\pi p) = (27.0 \pm 0.4)^- \text{mb} \text{ or } (25.2 \pm 0.4)^+ \text{mb} \text{ at } 10 \text{ GeV/c (reference 14),}$$

$$\sigma^{\text{tot}}(pp) = (39.9 \pm 1.5) \text{mb} \text{ at } 28 \text{ GeV/c (reference 15),}$$

where the "-" indicates π^-p scattering and the "+" indicates π^+p scattering. That these two cross sections are different indicates that the energy is not yet high enough for the Pommeranchuk theorem to hold. This theorem states that the cross sections should approach each other and approach a constant. If we pick, however, (25 ± 1) mb for $\sigma^{\text{tot}}(\pi p)$ and (40 ± 1.5) mb for $\sigma^{\text{tot}}(pp)$, then from Eq. (37) we obtain

$$\sigma^{\text{tot}}(\pi\pi) = (15.6 \pm 1.1) \text{ mb} . \quad (38)$$

The derivation here of the high-energy limit for $\sigma^{\text{tot}}(\pi\pi)$ is just an example of many similar predictions which can be made. Such arguments are all based upon the notion that the residues of Regge poles are factorable^{16,17} in the same way that the residues of elementary-particle poles in field theory are factorable.

X. ANGULAR DISTRIBUTIONS

Let us now consider angular distributions:

$$\frac{d\sigma^{\text{elas}}}{d\Omega} = |f|^2 = \left| \frac{2A(s, t)}{\sqrt{s}} \right|^2 , \quad (39)$$

in the high-energy limit.

From Eq. (31) we can see that $|A|^2$ behaves like s^{2a} as $s \rightarrow \infty$, so that Eq. (39) can be written

$$\frac{d\sigma^{\text{elas}}}{d\Omega} \rightarrow g(t) T_{\text{lab}}^{2a(t)-1} \text{ as } T_{\text{lab}} \rightarrow \infty , \quad (40)$$

with

$$s = (E_{\text{c. m.}}^{\text{tot}})^2 = (M_1 + M_2)^2 + 2T_{\text{lab}}^2 M_2 , \quad (41)$$

where M_1 and M_2 are the masses of the incident and target particles, respectively, T_{lab} is the kinetic energy of the incident particle in the lab frame, and $g(t)$ consists of constants and functional dependences on t . If we approximate $a(t)$ by the linear form

$$a(t) = a(0) + ta'(0) , \quad (42)$$

then Eq. (40) becomes

$$\frac{d\sigma^{\text{elas}}}{d\Omega} \rightarrow g(t) T_{\text{lab}}^{2a(0)-1} T_{\text{lab}}^{2ta'(0)} = g(t) T_{\text{lab}}^{2a'(0)-1} \exp[2a'(0)t \ln T_{\text{lab}}] . \quad (43)$$

Now recall that we are looking at a process in the s-channel where

$$t = -2q^2 (1 - \cos \theta). \quad (44)$$

The form of Eq. (43) is drawn in Fig. 9 where we note the exponential fall-off of the angular distribution as we go away from zero deg (t becoming more negative).

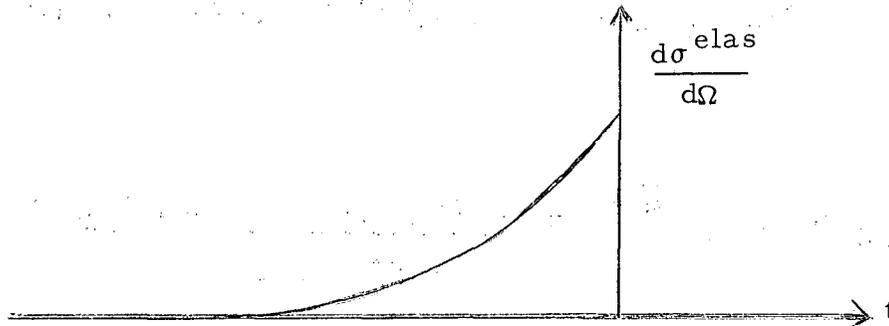


Fig. 9. Elastic-scattering cross section near 0 deg.

Note, also, that as T_{lab} increases the exponential falls off even faster with negative t . This is the logarithmic shrinking of the diffraction peak with high energy, which appears to be borne out by high-energy experiments at CERN^{12, 18, 19, 20}. This is to be compared with ordinary diffraction scattering where the width, when plotted against t , is constant (see Appendix B).

Equation (40) also gives us a method of determining $\alpha(t)$. Take the ratio of cross sections at two different laboratory energies and the same value of t . Then the function $g(t)$ cancels and we obtain¹²

$$\frac{d\sigma^{\text{elas}} [T_{\text{lab}}^{(1)}] / d\Omega}{d\sigma^{\text{elas}} [T_{\text{lab}}^{(2)}] / d\Omega} = \left[\frac{T_{\text{lab}}^{(1)}}{T_{\text{lab}}^{(2)}} \right]^{2\alpha(t)-1} \quad (45)$$

We can now solve for $\alpha(t)$ as a function of t . Once $\alpha(t)$ is known $g(t)$ can be determined.

XI. TOTAL ELASTIC CROSS SECTIONS

We can integrate Eq. (43) over t to obtain the total elastic cross section:

$$\begin{aligned} \sigma^{el} &= \int_{-1}^{+1} \frac{d\sigma^{el}}{d\Omega} d(\cos \theta) = \int_{-1}^{+1} g(t) s^{2\alpha(0)-1} \exp\{(\ln s) 2\alpha'(0) [2\vec{q}^2(1-z)]\} dz \\ &= g(0) s^{2\alpha(0)-1} s^{-4\vec{q}^2 a'} \frac{\exp(+4\vec{q}^2 a' \ln s) - \exp(-4a' \vec{q}^2 \ln s)}{-4\vec{q}^2 a' \ln s} \end{aligned} \quad (46)$$

where we have assumed that $g(t)$ is a slowly varying function. Since $(2\vec{q}_s)^2 \rightarrow s$ as $s \rightarrow \infty$, and assuming that $a' > 0$,

$$\sigma^{el} \rightarrow g(0) s^{2\alpha(0)-1-sa'(0)} \left[\frac{s^{a'(0)s}}{sa' \ln s} \right] \quad (47)$$

Recalling that $\alpha(0) = 1$, then Eq. (47) reduces to

$$\sigma^{el} \rightarrow \frac{g(0)}{a' \ln s} \quad (48)$$

Thus the elastic cross section goes logarithmically to zero in the limit of high energy. This is not surprising since it was shown that the width of the elastic angular distribution was shrinking logarithmically in s . This does not, however, contradict the fact that the total cross section tends to a constant at high energies; it means that total cross sections become pure inelastic in the limit of high energies. This contrasts with the prediction of ordinary diffraction scattering that

$$\sigma^{el} = \sigma^{inel} = \pi R^2 \quad (49)$$

in the same limit of high energies, R being the range of the interaction.

XII. ISOLATING REGGE TRAJECTORIES

We wish now to discuss Regge trajectories other than the Pomeron and their experimental implications.²¹

The various Regge poles that can occur in the t-channel depend upon the quantum numbers of the t-channel. For example, in pp scattering the t-channel is $\bar{p}p$ scattering. This t-channel state has the quantum numbers $S=0$, $B=0$, and $I=0$ or 1 , where S is the strangeness quantum number, B is baryon number, and I is the isotopic spin quantum number. The Regge trajectories that have these quantum numbers and can therefore contribute in the intermediate states are the Pomeron (P), second Pomeron (P'),^{22,23} ω , π , ρ , η .

In $\pi\pi$ scattering the initial state of the crossed channel (t-channel) is a two-pion state which has quantum numbers $S=0$, $B=0$, $I=0, 1$ or 2 and $G=+1$. (G is the eigenvalue of the G-parity operator; two pions must be in a state of even G-parity.) Since $I=2$ is not possible for the final state, $I=0$ or 1 are the possible intermediate states connecting $\pi\pi$ to $\bar{p}p$. A G of $+1$ excludes the π and the ω so that we are left with the first and second Pomeron, ρ , and η .

From the optical theorem we note that the total cross section is proportional to $\text{Im } A$, whereas the differential cross section $d\sigma/d\Omega$ is proportional to $|A|^2$. The fact that the former cross section is linear in the scattering amplitude allows one to obtain certain interesting relationships which will isolate the contributions of various Regge trajectories.

The following relationship between isotopic spin states will be useful in what follows:²⁴

$$\exp(+i\pi\mathfrak{I}_2) |I, I_3\rangle = \exp[-i\pi(I+I_3)] |I, -I_3\rangle. \quad (50)$$

Here I and I_3 are the eigenvalues of the total and third component of isotopic spin, respectively, and \mathfrak{I}_2 is the second component of the isotopic spin operator. \mathfrak{I}_2 will generally be represented as a matrix and $\exp(+i\pi\mathfrak{I}_2)$ is to be defined in terms of the power series expansion of the exponential. The operator $\exp(+i\pi\mathfrak{I}_2)$ rotates the state 180 deg about the "2" axis in isotopic spin space and also produces a phase factor $\exp[-i\pi(I+I_3)]$. It should be noted that Eq. (50) is equally true for single-particle or many-particle states. In the latter case the eigenstates and operators refer to the total isotopic spin of the combined system. We may in this case write

$$\exp(+i\pi\mathfrak{I}_2) = \exp(+i\pi \sum_j \mathfrak{I}_2^j) = \prod_j \exp(+i\pi\mathfrak{I}_2^j), \quad (51)$$

where j is the particle index. Thus the operator $\exp(+i\pi\mathfrak{I}_2)$ operating on the combined system may be factored into a sequence of operators which operate on the one-particle states.

We also note that the charge Q of a system is related to I_3 by

$$\frac{Q}{e} = I_3 + \frac{1}{2} (B + S).$$

So in systems where $Q = B = S = 0$ it follows that $I_3 = 0$ and Eq. (50) becomes

$$\exp(+i\pi\mathfrak{I}_2) |I, 0\rangle = \exp(-i\pi I) |I, 0\rangle = (-1)^I |I, 0\rangle. \quad (52)$$

Now let us consider π^+p scattering. The s -channel process is shown in Fig. 10.

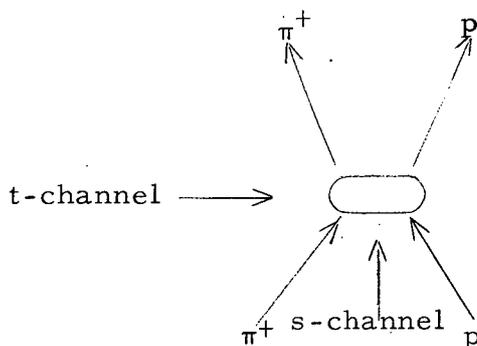


Fig. 10. Scattering of $\pi^+ + p \rightarrow \pi^+ + p$.

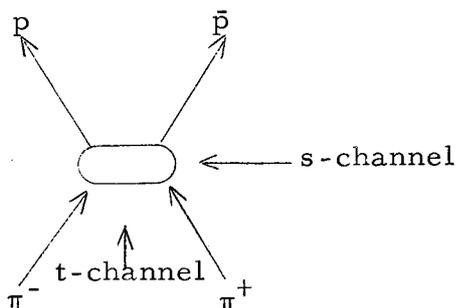


Fig. 11. t -channel of $\pi^+ + p \rightarrow \pi^+ + p$.

We now operate on the initial state of Fig. 11 (the t -channel,) with

$$R_2 = \exp(+i\pi\mathfrak{I}_2) = \exp(+i\pi\mathfrak{I}_2^-) \exp(+i\pi\mathfrak{I}_2^+). \quad (53)$$

The superscripts (-) and (+) denote π^- and π^+ , respectively. We find from Eq. (50) that

$$\exp(+i\pi\mathfrak{I}_2^-) |\pi^-\rangle = |\pi^+\rangle; \quad \exp(+i\pi\mathfrak{I}_2^+) |\pi^+\rangle = |\pi^-\rangle; \quad (54)$$

so from Eq. (53) we obtain

$$R_2 |\pi^-\pi^+\rangle = |\pi^+\pi^-\rangle. \quad (55)$$

But we can also write from Eq. (52) that

$$R_2 |\pi^- \pi^+\rangle = (-1)^I |\pi^- \pi^+\rangle \quad (56)$$

This last equation is to be understood in the sense that we have expanded the state $|\pi^- \pi^+\rangle$ in terms of eigenstates of total isotopic spin and the operator R_2 multiplies each eigenstate by $(-1)^I$. (Here we have used the fact that $B=S=Q=I_3=0$ for the $\pi^+\pi^-$ system.) We combine the last two equations and represent these remarks diagrammatically in Fig. 12.

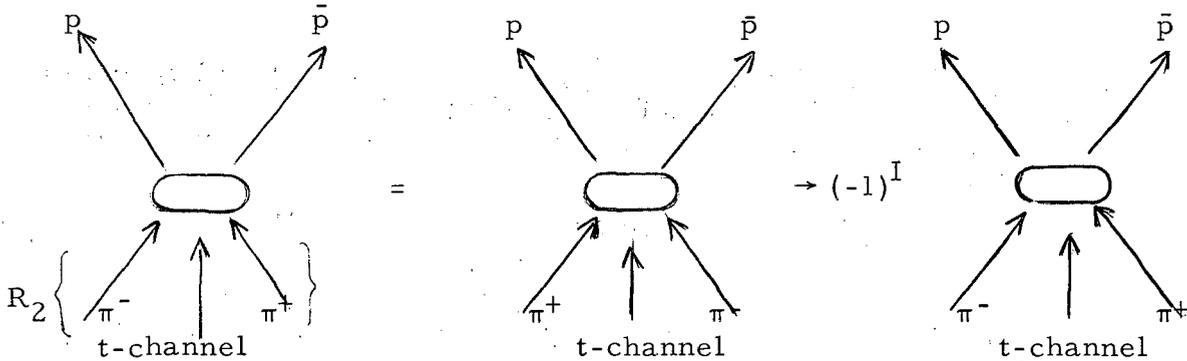


Fig. 12. Diagrammatical representation of the effect of an isotopic-spin rotation. The $(-1)^I$ term to the right is understood as a factor occurring in the isotopic-spin expansion of the $\pi^- \pi^+$ state.

In Fig. 13 we look at the process from the point of view of the s-channel.

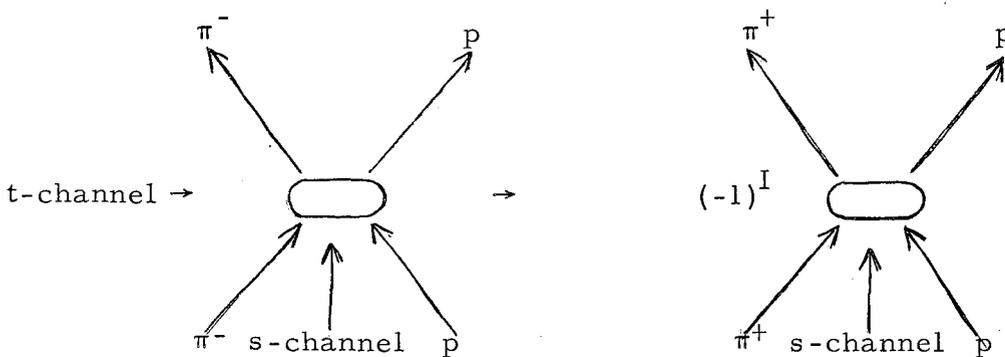


Fig. 13. Diagrammatical representation of the effect in the s-channel ($\pi^+ p$ scattering) of an isotopic-spin rotation in the t-channel.

It follows from what has been said that $A_{\pi^+ p}^+(s, t) + A_{\pi^- p}^-(s, t)$ contains only pure $I=0$ in the t-channel and $A_{\pi^+ p}^+(s, t) - A_{\pi^- p}^-(s, t)$ contains only pure $I=1$ in

the t-channel. The states in the t-channel must also have $B=0$, $S=0$, $G=+1$. From the optical theorem,

$$\sigma^{\text{tot}} \propto \frac{\text{Im } A(s, 0)}{q_s \sqrt{s}}, \quad (57)$$

and we have seen that

$$\sigma^{\text{tot}} \propto \sum_{i \rightarrow \infty} b_i(0) (s)^{a_i(0)-1}. \quad (58)$$

[See Eq. (35).] If we consider $\sigma^{\text{tot}}(\pi^+p) + \sigma^{\text{tot}}(\pi^-p)$ only $I=0$ Regge pole terms will be present. When considering $\sigma^{\text{tot}}(\pi^+p) - \sigma^{\text{tot}}(\pi^-p)$, only $I=1$ Regge pole terms will be present. In the latter case the leading behavior at high energy will be

$$\sigma^{\text{tot}}(\pi^+p) - \sigma^{\text{tot}}(\pi^-p) \propto b_\rho(0) (s)^{a_\rho(0)-1}, \quad (59)$$

since the ρ trajectory is the highest trajectory with $I=1$. The combination $\sigma^{\text{tot}}(\pi^+p) + \sigma^{\text{tot}}(\pi^-p)$ will be dominated by the Pomeron.

Another interesting combination of cross sections is that of pp and np (see Fig. 14).²⁵ The R_2 operator operating on the initial state of the t-channel of the pp system gives a relationship between amplitudes analogous to Fig. 12.²⁶

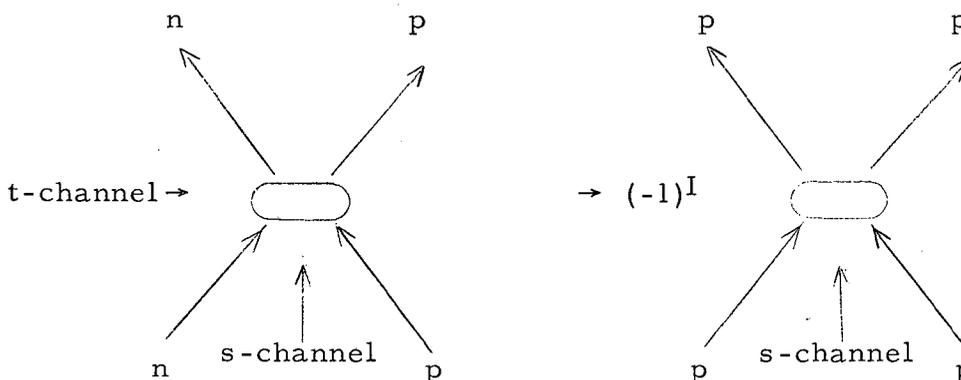


Fig. 14. Diagrammatical representation of the effect in the s-channel (pp scattering) of an isotopic-spin rotation in the t-channel.

Therefore the high-energy limit of the combination $\sigma^{\text{tot}}(pp) - \sigma^{\text{tot}}(np)$ is controlled by $I=1$ Regge poles. The quantum numbers of this t-channel must then be $S=0$, $B=0$, $I=1$. The highest Regge trajectory with these quantum numbers is the ρ , so that this combination of cross sections should be dominated by

$$\sigma^{\text{tot}}(pp) - \sigma^{\text{tot}}(np) \propto s^{a_\rho(0)-1} \text{ as } s \rightarrow \infty. \quad (60)$$

Since $\alpha_P(0)$ is 1 and all other Regge trajectories are below it, then $\alpha_P(0) < 1$ and the cross section difference (60) tends to zero. How it tends to zero is given by Eq. (60). The combination $\sigma^{\text{tot}}(pp) + \sigma^{\text{tot}}(np)$ is pure $I=0$ exchange. The leading behavior at high energies is given by the Pomeron and the sum approaches a constant.

Additional relations can be obtained from the G-parity operator,²⁷

$$\mathcal{G} = C R_2, \quad (61)$$

where C is the charge conjugation operator. The eigenvalue of the operator, G , is either ± 1 . In analogy with the development leading to Eqs. (55) and (56), we write (starting with the t-channel of pp scattering)²⁶

$$\mathcal{G} R_2 |\bar{p}p\rangle = \mathcal{G} |\bar{n}n\rangle = |p\bar{p}\rangle \quad (62)$$

but also

$$\mathcal{G} R_2 |\bar{p}p\rangle = G(-1)^I |\bar{p}p\rangle, \quad (63)$$

where again the interpretation of Eq. (63) is that the t-channel $\bar{p}p$ state is expanded in terms of eigenstates of total isotopic spin and G-parity, and the operator $\mathcal{G} R_2$ multiplies the eigenstates in the sum by $G(-1)^I$. Figure 15 illustrates this relationship.

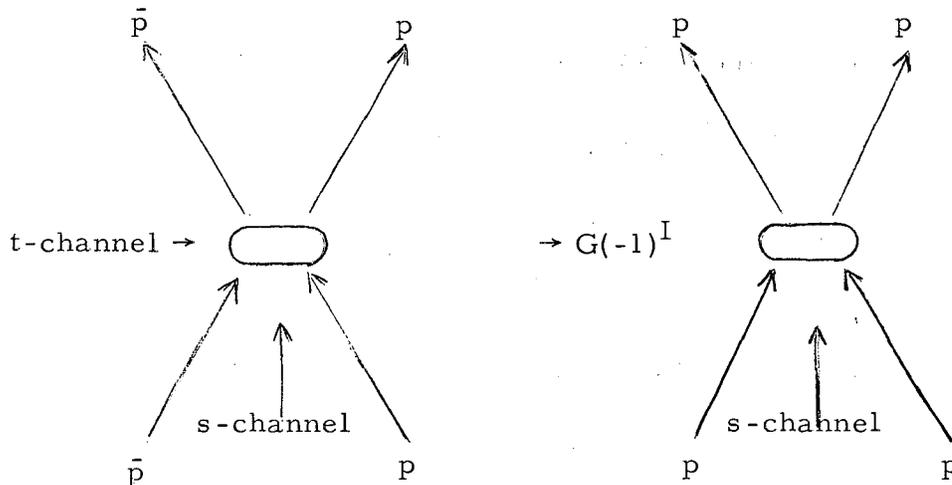


Fig. 15. Diagrammatical representation of the effect in the s-channel (pp scattering) of an isotopic-spin rotation and a G-conjugation in the t-channel.

From the above we see that $\sigma^{\text{tot}}(pp) - \sigma^{\text{tot}}(p\bar{p})$ contains the effects of systems exchanged in the t-channel with quantum numbers either (a) $G = -1$ and $I = 0$ or (b) $G = +1$ and $I = 1$. A possible Regge trajectory which would dominate the former state would be the ω , whereas the ρ fits the quantum numbers for the latter case.

Another possibility is to operate with just \mathcal{G} and to sift out states of well-defined G-parity. For example, we can start with np scattering (see Fig. 16).

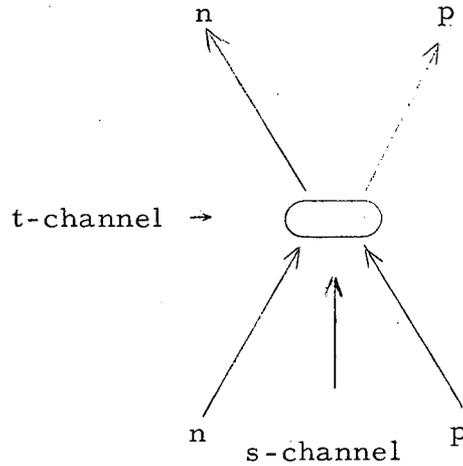


Fig. 16. Scattering of $n + p \rightarrow n + p$.

We operate on the t-channel $\bar{n}n$ state with \mathcal{G} ,

$$\mathcal{G} |\bar{n}n\rangle = |p\bar{p}\rangle \quad (64)$$

and also

$$\mathcal{G} |\bar{n}n\rangle = G |\bar{n}n\rangle ; \quad (65)$$

then we obtain the relationships shown in Fig. 17.

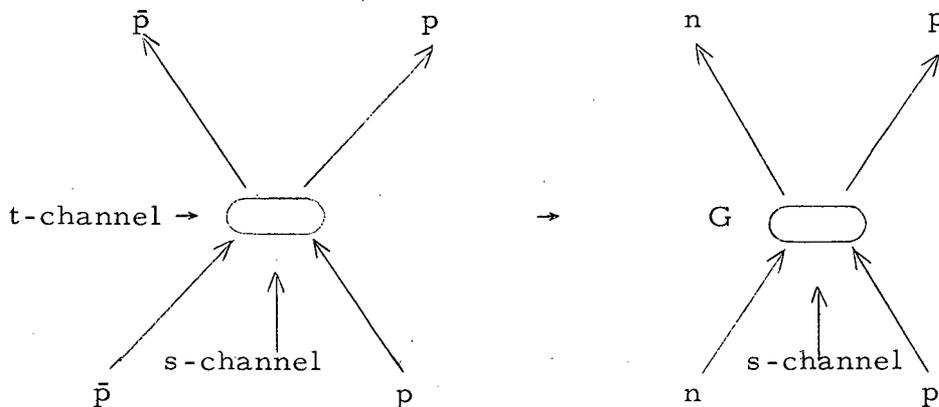


Fig. 17. Effect of G-conjugation on the t-channel of np scattering.

Thus the difference $\sigma^{\text{tot}}(\text{np}) - \sigma^{\text{tot}}(\text{p}\bar{\text{p}})$ is controlled at high energies by Regge poles of negative G-parity, so that either the ω or the π might contribute to this difference of cross sections.²⁸

We summarize the results of this section in Table I.

Table I. High-energy behavior of total cross sections.^a

Cross sections	Contributing Regge poles	Expected high-energy behavior
$\sigma^{\text{tot}}(\pi^+ \text{p}) + \sigma^{\text{tot}}(\pi^- \text{p})$	P, P', b	$a + bs$ $[a_{P'}(0) - 1]$
$\sigma^{\text{tot}}(\pi^+ \text{p}) - \sigma^{\text{tot}}(\pi^- \text{p})$	ρ	cs $[a_\rho(0) - 1]$
$\sigma^{\text{tot}}(\text{pp}) + \sigma^{\text{tot}}(\text{np})$	P, P', ω^b	$d + es$ $[a_{P'}(0) - 1]$ $+fs$ $[a_\omega(0) - 1]$
$\sigma^{\text{tot}}(\text{pp}) - \sigma^{\text{tot}}(\text{np})$	ρ	gs $[a_\rho(0) - 1]$
$\sigma^{\text{tot}}(\text{pp}) + \sigma^{\text{tot}}(\bar{\text{p}}\text{p})$	P, P', b	$d + es$ $[a_{P'}(0) - 1]$
$\sigma^{\text{tot}}(\text{pp}) - \sigma^{\text{tot}}(\bar{\text{p}}\text{p})$	ρ, ω	fs $[a_\omega(0) - 1]$ $+gs$ $[a_\rho(0) - 1]$
$\sigma^{\text{tot}}(\text{np}) + \sigma^{\text{tot}}(\text{p}\bar{\text{p}})$	P, P', ρ^b	$d + es$ $[a_{P'}(0) - 1]$ $-gs$ $[a_\rho(0) - 1]$
$\sigma^{\text{tot}}(\text{np}) - \sigma^{\text{tot}}(\text{p}\bar{\text{p}})$	ω	fs $[a_\omega(0) - 1]$

^a We have not included in our discussion the conjectured P'' or ABC particle [N. E. Booth, A. Abashian, K. M. Crowe, Phys. Rev. Letters 7, 35 (1961)]. If it were included, it would contribute to the same cross-section combinations as P and P' .

^b The η does not appear in these places for the same reason that the π does not sometimes appear, as explained in reference 28.

A table of this type was first constructed by Udgoankar.²¹ We have not exhausted the possible predictions and the reader can easily enlarge the table.

XIII. BACKWARD AND CHARGE-EXCHANGE SCATTERING

In the previous section we have seen various methods of obtaining the position of the Regge poles at $t = 0$. The method involved used the optical theorem, which connects the total cross section linearly with the scattering amplitude. However, the theorem is only valid for $t = 0$. To obtain the value for $a(t)$ at $t \neq 0$ we look at the differential elastic scattering cross section. From Eqs. (1) and (4)

$$\frac{d\sigma}{d\Omega} = |f|^2 = \frac{4 |A(s, t)|^2}{s} \quad (66)$$

and, taking the proper symmetric combination of Legendre polynomials from Eq. (26), we have

$$\frac{d\sigma}{d\Omega} = \frac{4 \left| \sum_i \pi(2a_i+1) \beta_i(t) [P_{a_i}(z) \pm P_{a_i}(-z)] / 2 \sin \pi a_i(t) \right|^2}{s} \quad (67)$$

$$\frac{d\sigma}{d\Omega} \rightarrow \frac{\left| \sum_i c_i(t) s^{a_i(t)} \right|^2}{s} \quad (\text{as } s \rightarrow \infty) \quad (68)$$

For t near zero we have seen that (68) is dominated by a peak whose width in t shrinks logarithmically with incident laboratory energy, and that this behavior for elastic scattering is dominated by the Pomeranchon, [see Eq. (43)].

If we look at scattering near 180 deg, however, the Pomeranchon no longer dominates so that we can discover the behavior of $a(t)$ vs t for other trajectories. Of course we must discuss a case which has nonidentical particles so that 180 deg can be distinguished from 0 deg. Consider π^+p elastic scattering in the backward direction. To avoid introducing the third or u-channel, we redraw the s-channel diagram of Fig. 10 in Fig. 18.

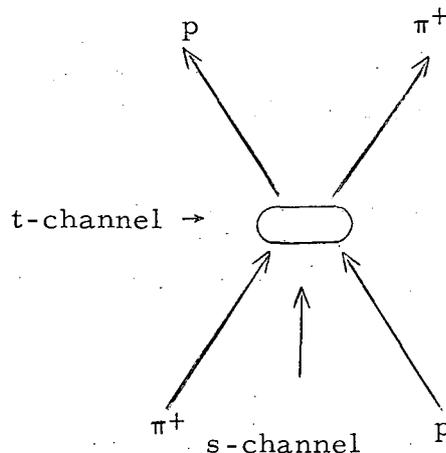


Fig. 18. Backward π^+p scattering.

We see that in the t-channel of this diagram, I can be either 1/2 or 3/2, S=0, B=1 so that the possible trajectories that could contribute are the nucleon or the 3,3 resonance. The latter looks as if it is above the nucleon resonance so that it should dominate.

A more interesting cross section would be the π^-p system which in the cross-channel of Fig. 19

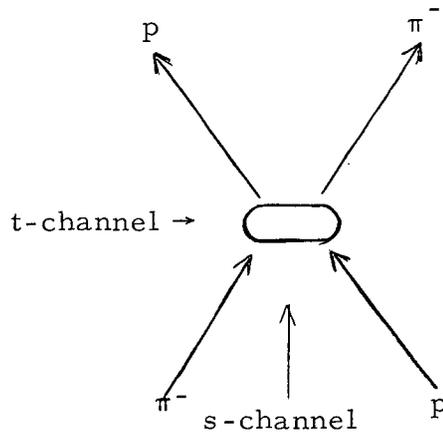


Fig. 19. Backward π^-p scattering.

is a pure $I = 3/2$ state. The only trajectory that could contribute here is, then, the $3,3 N^*$ resonance. Its behavior would be given, then, by

$$\frac{d\sigma^{elas}}{d\Omega} (\pi^-p \rightarrow \pi^-p \text{ near } 180 \text{ deg}) \rightarrow g(t) s^{2\alpha_{N^*}(t)-1} \quad (69)$$

Consider π^-p charge exchange scattering (Fig. 20).

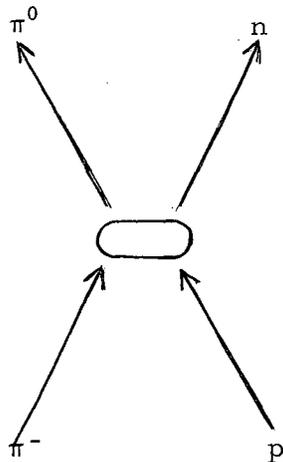


Fig. 20. Charge-exchange scattering.

The crossed channel of this reaction is pure: $I = 1$, $G = +1$, $S = 0$, $B = 0$, which would then be controlled by the ρ -meson Regge trajectory.

APPENDIX A. EXCHANGE SCATTERING²⁹

An exchange potential scatters two particles like an ordinary potential and in addition exchanges the positions of the particles. Mathematically we can write an exchange potential as $PV_E(r)$, which, by operating on the wave function, gives

$$PV_E(r)\psi(\vec{r}) = V_E(r)\psi(-\vec{r}), \quad (\text{A-1})$$

where P is an operator which acts on the wave function to change the direction of the relative-position vector \vec{r} between two particles. If we change \vec{r} to $-\vec{r}$ we have essentially interchanged the positions of the two particles. The most general potential that we can write down in potential theory is

$$V(r) = V_D(r) + PV_E(r), \quad (\text{A-2})$$

where the subscript D stands for the direct potential and E the exchange potential. Now how would one solve the Schrödinger equation with this general potential in it?

Rewrite Eq. (A-2) as

$$V(r) = \frac{1+P}{2} (V_D + V_E) + \frac{1-P}{2} (V_D - V_E). \quad (\text{A-3})$$

Let us write a most general wave function $\psi(r)$ which can always be broken into two parts, one an even function of \vec{r} and the other an odd function of \vec{r} :

$$\psi(\vec{r}) = \psi_e(\vec{r}) + \psi_o(\vec{r}), \quad (\text{A-4})$$

where

$$\begin{aligned} \psi_e(-\vec{r}) &= \psi_e(\vec{r}), \\ \psi_o(-\vec{r}) &= -\psi_o(\vec{r}). \end{aligned} \quad (\text{A-5})$$

Since $P\psi(\vec{r}) = \psi(-\vec{r})$ it is seen that

$$\frac{1+P}{2} \psi(\vec{r}) = \psi_e(\vec{r}) \quad (\text{A-6})$$

and

$$\frac{1-P}{2} \psi(\vec{r}) = \psi_o(\vec{r}). \quad (\text{A-7})$$

These considerations show that one can solve the Schrödinger equation

$$H\psi = i\hbar \frac{\partial \psi}{\partial t} \quad (\text{A-8})$$

by breaking it into two uncoupled equations,

$$H_e \psi_e = i\hbar \frac{\partial \psi_e}{\partial t} \quad (\text{A-9})$$

and

$$H_o \psi_o = i\hbar \frac{\partial \psi_o}{\partial t}, \quad (\text{A-10})$$

where

$$H_e = \frac{p^2}{2m} + (V_D + V_E), \quad (\text{A-11})$$

$$H_o = \frac{p^2}{2m} + (V_D - V_E). \quad (\text{A-12})$$

Thus in the presence of an exchange potential the even and odd states scatter independently.

APPENDIX B. ORDINARY DIFFRACTION SCATTERING

The width of an ordinary diffraction peak is proportional to λ/R , where R is the radius of the black body. Replacing λ by \hbar/q we have the angular width of diffraction scattering as

$$\Delta\theta \propto 1/qR.$$

For small angles, $\cos\theta \approx 1 - (\theta^2/2)$, so the value of t at the minimum of the ordinary diffraction peak (which we will call τ) is

$$\theta = -2\vec{q}^2 (1 - \cos\theta) \approx -\frac{\vec{q}^2}{q^2} R^2 = \text{constant}.$$

This behavior of ordinary diffraction scattering is to be contrasted with the behavior as predicted by Eq. (43).

REFERENCES

1. T. Regge, *Nuovo Cimento* 14, 951 (1959).
2. T. Regge, *Nuovo Cimento* 18, 947 (1960).
3. G. F. Chew and S. C. Frautschi, *Phys. Rev. Letters* 7, 394 (1961).
4. G. F. Chew and S. C. Frautschi, *Phys. Rev. Letters* 8, 41 (1962).
5. S. Mandelstam, to be published.
6. G. F. Chew, *S-Matrix Theory of Strong Interactions* (W. A. Benjamin Inc., New York, 1961).
7. E. J. Squires, *Nuovo Cimento* 25, 242 (1962).
8. A. Ahmadzadeh, P. G. Burke, and C. Tate, Lawrence Radiation Laboratory Reports UCRL-10140, March 1962, and UCRL-10216 May 1962 (both unpublished).
9. A. Sommerfeld, *Partial Differential Equations in Physics* (Academic Press, Inc., New York, 1949), p. 279.
10. Actually the asymptotic behavior of the Legendre polynomials includes some constant factors and factors with inconsequential α dependence. We shall assume that such factors are absorbed in $\beta_i(t)$ in what follows.
11. J. R. Taylor, *Phys. Rev.* 127, 2257 (1962).
12. S. C. Frautschi, M. Gell-Mann, and F. Zachariasen, *Phys. Rev.* 126, 2204 (1962).
13. Regge trajectories for half-integral spin particles are also conjectured to define a particle or resonance state only at every other half-integral value of angular momentum J . For example, the nucleon trajectory may be a particle or resonance state only at $J=1/2, 5/2, 9/2, \dots$. It is also assumed that in scattering particles with spin, Regge poles occur in the total-angular-momentum variable J . [See references 3, 4, 10, as well as R. Blankenbecler and M. L. Goldberger, *Phys. Rev.* 126, 766 (1962).]
14. G. Van Dardel, R. Mermod, P. A. Piroué, M. Virargent, G. Weber, K. Winter, *Phys. Rev. Letters* 7, 127 (1961).
15. A. Ashmore, G. Cocconi, A. N. Diddens, A. M. Wetherell, *Phys. Rev. Letters* 5, 576 (1960).
16. M. Gell-Mann, *Phys. Rev. Letters* 8, 263 (1962).
17. J. Charap and E. J. Squires, Lawrence Radiation Laboratory Report UCRL-10115, March 1962.
18. A. N. Diddens, E. Lillethun, G. Manning, A. E. Taylor, T. G. Walker and A. M. Wetherell, *Phys. Rev. Letters* 9, 111 (1962).
19. A. N. Diddens, E. Lillethun, G. Manning, A. E. Taylor, T. G. Walker, and A. M. Wetherell, *Phys. Rev. Letters* 9, 108 (1962).
20. F. Hadyioannou, R. J. N. Phillips and W. Rarita, *Phys. Rev. Letters* 9, 183 (1962).
21. B. M. Udgoankar, *Phys. Rev. Letters* 8, 142 (1962).

- 22. K. Igi, Phys. Rev. Letters 9, 76 (1962).
- 23. K. Igi, Two Vacuum Poles and Pion-Nucleon Scattering (to be published).
- 24. A. R. Edmonds, Angular Momentum in Quantum Mechanics, (Princeton University Press, Princeton, New Jersey, 1957), p. 55.
- 25. For a detailed study of the effect of Regge trajectories in nucleon-nucleon scattering see I. J. Muzinich (Ph. D. Thesis), High-Energy Nucleon-Nucleon Scattering, Lawrence Radiation Laboratory Report UCRL-10331, June 1962 (unpublished).

26. Recall that

$$R_2 \begin{pmatrix} |p\rangle \\ |n\rangle \\ |\bar{n}\rangle \\ |\bar{p}\rangle \end{pmatrix} = \begin{pmatrix} -|n\rangle \\ |p\rangle \\ |\bar{p}\rangle \\ -|\bar{n}\rangle \end{pmatrix} \text{ and } \begin{pmatrix} |p\rangle \\ |n\rangle \\ |\bar{n}\rangle \\ |\bar{p}\rangle \end{pmatrix} = \begin{pmatrix} -|\bar{n}\rangle \\ |\bar{p}\rangle \\ |p\rangle \\ -|n\rangle \end{pmatrix}$$

(See reference 27).

- 27. T. D. Lee and C. N. Yang, Nuovo Cimento 3, 749 (1956).
- 28. It turns out that only triplet states in the t ($N\bar{N}$) channel contribute to the total cross section. The π cannot match the quantum numbers of a triplet $N\bar{N}$ system, so actually the π trajectory does not contribute to this total cross-section difference. (See reference 25.)
- 29. Blatt and Weisskopf, Theoretical Nuclear Physics (John Wiley & Sons, Inc., New York, 1952), p. 127.

This report was prepared as an account of Government sponsored work. Neither the United States, nor the Commission, nor any person acting on behalf of the Commission:

- A. Makes any warranty or representation, expressed or implied, with respect to the accuracy, completeness, or usefulness of the information contained in this report, or that the use of any information, apparatus, method, or process disclosed in this report may not infringe privately owned rights; or
- B. Assumes any liabilities with respect to the use of, or for damages resulting from the use of any information, apparatus, method, or process disclosed in this report.

As used in the above, "person acting on behalf of the Commission" includes any employee or contractor of the Commission, or employee of such contractor, to the extent that such employee or contractor of the Commission, or employee of such contractor prepares, disseminates, or provides access to, any information pursuant to his employment or contract with the Commission, or his employment with such contractor.

